Article

Initiation, Elongation, and Termination of Bacterial Cellulose Synthesis

John B. McManus,[†] Hui Yang,[‡] Liza Wilson,[‡] James D. Kubicki,[§] and Ming Tien*,[†]

[†]Department of Biochemistry and Molecular Biology and [‡]Department of Biology, The Pennsylvania State University, University Park, Pennsylvania 16802, United States

[§]Department of Geological Sciences, University of Texas at El Paso, El Paso, Texas 79968, United States

S *Supporting Information*

ABSTRACT: Cellulose is the major component of the plant cell wall and composed of β-linked glucose units. Use of cellulose is greatly impacted by its physical properties, which are dominated by the number of individual cellulose strand within each fiber and the average length of each strand. Our work described herein provides a complete mechanism for cellulose synthase accounting for its processivity and mechanism of initiation. Using ionic liquids and gel permeation chromatography, we obtain kinetic constants for initiation, elongation, and termination (release of the cellulose strand from the enzyme) for two bacterial cellulose synthases (*Gluconacetobacter hansenii* and *Rhodobacter sphaeroides*). Our results show that initiation of synthesis is primer-independent.

After initiation, the enzyme undergoes multiple cycles of elongation until the strand is released. The rate of elongation is much faster than that of steady-state turnover. Elongation requires cyclic addition of glucose (from uridine diphosphate-glucose) and then strand translocation by one glucose unit. Translocations greater than one glucose unit result in termination requiring reinitiation. The rate of the strand release, relative to the rate of elongation, determines the processivity of the enzyme. This mechanism and the measured rate constants were supported by kinetic simulation. With the experimentally determined rate constants, we are able to simulate steady-state kinetics and mimic the size distribution of the product. Thus, our results provide for the first time a mechanism for cellulose synthase that accounts for initiation, elongation, and termination.
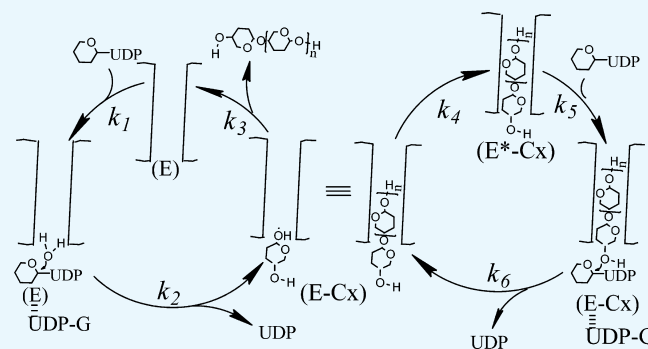
INTRODUCTION

Cellulose is a polymer of β-1,4 linkage glucose (Glc) units. It is the major component of plant cell walls[1] and thus the most abundant renewable polymer on earth.[2,3] Cellulose strands can vary from hundreds to thousands of glucose units in length.[4−8] Because of the extensive hydrogen bonding interactions of individual strands, cellulose exists as microfibrils making it an excellent structural component for the plant cell wall.[1] A key property of cellulose is the degree of polymerization (DOP). Higher DOP values are favorable for use of cellulose as fabric or paper, whereas lower DOPs are favorable for digestibility (bioethanol).[6] DOP measurements can be made through linkage analysis (number of glucose units per nonreducing end), viscosity measurement,[5] or by gel permeation chromatography (GPC),[9] once the individual strands have been separated and solubilized.

The DOPs of cellulose of different sources vary.[4−8] Although not proven, it is thought to be an intrinsic property of an enzyme's processivity, which is defined as average number of glucose units added to the growing polymer before the strand is released (termination). Cellulose is made by both plants and microbes. The source of each cellulose chain is the enzyme, cellulose synthase. The plant enzyme has eluded purification, however, two bacterial enzymes, *Gluconacetobacter hansenii*[10,11] and *Rhodobacter sphaeroides*,[12] have been purified to homogeneity. The most extensively studied bacterial system is of *G. hansenii*. The first crystal structure was obtained with the enzyme from *R. sphaeroides*.[12−15] To date, no studies have examined the DOP of enzyme-synthesized cellulose or the kinetics of the process. Synthesis of any polymer entails initiation, elongation, and termination (strand release).

In the present study, we perform kinetic and chemical analyses of cellulose synthesized by two purified bacterial enzymes, AcsA-AcsB from *G. hansenii* and BcsA-BcsB from *R. sphaeroides*. Ionic liquids are used to solubilize the newly synthesized cellulose, which enables analysis by GPC and multiangle laser light scattering (MALLS). Using uridine diphosphate (UDP)-[¹⁴C]-glucose as the substrate, we are then able to determine the amount of cellulose synthesized at each DOP size range. From these studies, we provide a kinetic account for processivity. With the mechanism and the

measured rate constants, we are able to simulate both steady-state kinetics and processivity with Kinsim.[16]

■ RESULTS

GPC Analysis of Cellulose. Bacterial cellulose from *G. hansenii* has been characterized to be more crystalline than plant cellulose.[17−19] Using GPC and nitrated cellulose, the average DOP of the cellulose isolated from live cultures was measured to be 11 000−16 800.[20] However, there are only limited studies on in vitro-synthesized cellulose. The DOP of cellulose synthesized from a purified cellulose synthase BcsA-BcsB from *R. sphaeroides* had a measured DOP of 200−300.[12] This average, however, provides no details on the size distribution. To determine this size distribution, the enzymatically generated cellulose was carbanilated and then solubilized for analysis by GPC. Figure 1 shows the GPC profiles for
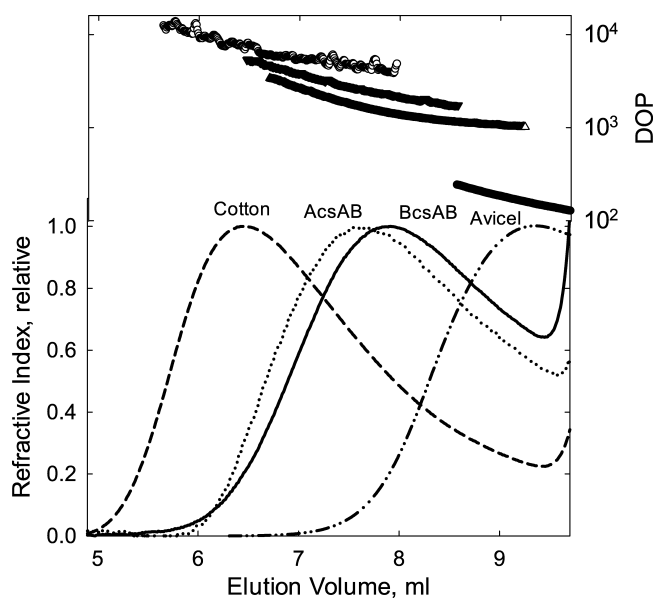

Figure 1. GPC elution profiles of cellulose tricarbanilates. Cellulose samples (as labeled in the figure) were carbanilated, as described in Materials and Methods. For cellulose synthesized from BcsA-BcsB or AcsA-AcsB, 0.5 μM enzyme with 5 mM UDP-Glc in a reaction volume of 1.0 mL was used, as described in Materials and Methods. Reactions were allowed to proceed for 12 h. A KD-806M column was used with tetrahydrofuran as the mobile phase at a flow rate of 0.5 mL min^{-1}. The figure shows the molecular weight distribution, converted to DOP on the right axis, above the associated refractive index detection signal.

cellulose synthesized from the two purified bacterial enzymes (*G. hensenii* and *R. sphaeroides*), Avicel, and cotton cellulose. Detection of the cellulose was via multiangle light scattering (MALLS), which provides information on the cellulose size. These results show that the cotton cellulose is largest with a peak DOP of 7800 and a maximum DOP of approximately 20 000 and the Avicel smallest with a peak DOP of 170. The bacterial cellulose size distribution is in between cotton and Avicel; cellulose synthesized by AcsA-AcsB is larger at a peak DOP of 2900 than that from BcsA-BcsB, which has a peak DOP of 1600.

Initiation: Reducing End Analysis. Cellulose synthase is a processive glycosyl transferase, where synthesis occurs at the nonreducing end with the 4-carbon hydroxyl attacking the anomeric carbon of UDP-glucose (UDP-Glc). Primer requirements are difficult to assess because as-purified heterologously

expressed *R. sphaeroides* cellulose synthase already contains a cellulose chain in the exit channel of the enzyme.[13] Thus, to examine whether initiation is dependent upon a primer, we utilized UDP-[14C]-Glc. If UDP-Glc is able to initiate primer-independent synthesis, then the reducing end should be 14C-labeled in UDP-[14C]-Glc-containing incubations. To examine this possibility, cellulose from such incubations with AcsA-AcsB or BcsA-BcsB was covalently modified at the reducing end with the fluorescent modifying agent 2-aminobenzamide (2AB).[21] The 2AB-modified cellulose was then hydrolyzed with cellulases and β-glucosidase producing free glucose and 2AB-labeled glucose. The 2AB-modified cellulose is easily separated from free glucose by reversed-phase chromatography. An internal standard of nonradioactive 2AB-glucose was added to the sample and the sample was separated by C-18 reversed-phase high-performance liquid chromatography (HPLC). 2AB-glucose is detected by its fluorescence. Glucose eluted as a major radioactive peak at ∼2.5 mL (Figure 2A,B). Another radioactive peak eluted at ∼13 mL, which co-elutes with the 2AB-glucose standard. The second fluorescent peak in Figure 2 is unreacted 2AB. These results, with both enzymes showing 14C-glucose at the reducing end, are consistent with primer-independent synthesis.

We also investigated whether formation of 14C-labeled reducing ends was derived from contaminating cellulase activity; however, this possibility was eliminated. Incubation of presynthesized cellulose with purified enzyme caused no change in the DOP (not shown).

Initiation: UDP-Glc Hydrolase Activity. A possible primer-independent mechanism involves UDP-Glc hydrolysis, yielding glucose, which then can enter the channel as the new reducing end. Indeed, free glucose was detected using glucose oxidase from UDP-Glc-containing incubations with BcsA-BcsB (Figure 2C). Nucleotide-sugar hydrolysis is a known activity of glycosyl transferases.[22,23]

Elongation: GPC DOP Analysis. Elongation involves multiple rounds of glucose addition from UDP-Glc. Little is known on the basis of how plants or microbes synthesize cellulose of different DOPs. Previously, DOP determinations of in vitro-synthesized cellulose by BcsA-BcsB yielded a numerical average of 200−300[12] and no information of size distribution. To determine the distribution, we used UDP-14C-Glc to label the cellulose, then solubilized the cellulose with dimethylacetamide containing 8% lithium chloride,[24,25] and analyzed by GPC. MALLS and a differential refractive index detector[9] were used to determine the DOP of the cellulose. BcsA-BcsB-synthesized cellulose (Figure 3A) showed a progressive increase in strand length up to 30 min, where the strand length reached a maximum of ∼11 700 (DOP at the peak is ∼1500). From 30 min to 4 h, the maximum cellulose size did not increase beyond DOP of ∼11 700. Notably, throughout the time course, the amount of smaller strands continued to increase. The same trend (increase in size to a maximum) was observed with AcsA-AcsB incubations except that the maximum DOP is larger at ∼23 100 (Figure 3B). The DOP at the peak is ∼3000. Thus, both enzymes exhibit an intrinsic processivity limit (Figure 3A,B).

The elution profiles also provided data for rate measurements. Total glucose incorporated versus time is plotted in Figure 3 (insets). The rate of cellulose synthesis can be calculated from the slopes of the lines in the insets yielding 1.4 s^{-1} for AcsA-AcsB and 0.37 s^{-1} for BcsA-BcsB (Figure 3, insets). These values, which were determined under saturating
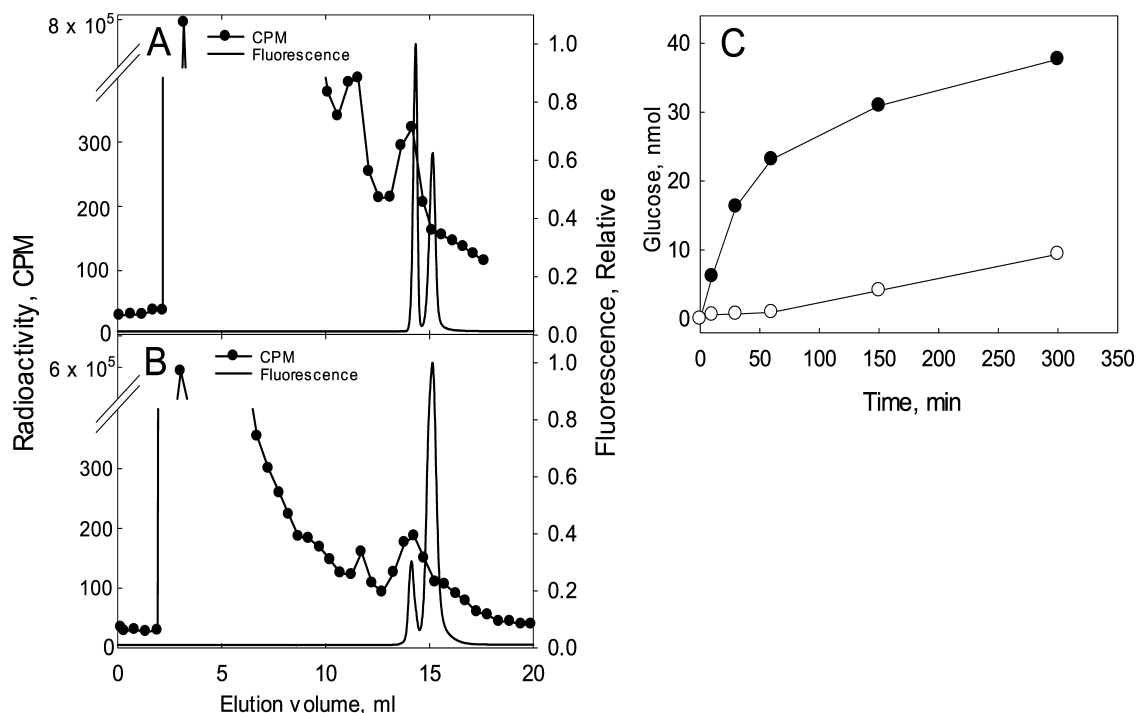
Figure 2. Chemical analysis of reducing ends generated by AcsA-AcsB (A) or BcsA-BcsB (B) and detection of glucose from BcsA-BcsB incubation (C). Cellulose was synthesized by either AcsA-AcsB (A) or BcsA-BcsB (B). Reaction mixtures and modification of the reducing end by 2AB and subsequent chromatography is described in Materials and Methods. Fractions of 0.5 mL were collected and quantified by scintillation spectroscopy. Nonradioactive 2AB-modified glucose was added to the reaction mixture. Note the split axis in the figure. (C) BcsA-BcsB-dependent generation of glucose from UDP-Glc as measured by glucose oxidase. Incubations contained 3 μM BcsA-BcsB and 5 mM UDP-Glc in a total volume of 0.3 mL as described in Materials and Methods with (●) or without (○) 10 μM cyclic-di-GMP. Aliquots were removed at specified times and glucose content measured by glucose oxidase.

conditions for UDP-Glc are close to the k_{cat} values of 1.7 ± 0.36 s^{-1} (AcsA-AcsB) (Figure 4A)[11] and 0.43 ± 0.17 s^{-1} (BcsA-BcsB) (Figure 4B) determined by the Michaelis−Menten equation.

Elongation: Rate of Elongation. The elution profiles (Figure 3) show that at the 2 min time point, the highest DOP (size of cellulose at the front of the elution profile) is ∼10 000 for AcsA-AcsB and ∼1500 for BcsA-BcsB. The rate of elongation can be calculated by dividing this DOP by the time (2 min), which yields a rate of glucose incorporation of 83 s^{-1} for AcsA-AcsB and 13 s^{-1} for BcsA-BcsB. This represents the rate at which glucose is being incorporated into an actively elongating cellulose chain. Its measurement must be taken during early time points of the incubation such that a population of the enzymes have yet to reach their processivity limit. We then measured the elongation rate in this way at various UDP-Glc concentrations. Saturation kinetics was observed for both enzymes (Figures S1A,B) with a maximum elongation rate (k_{cat}) of 12 s^{-1} and a k_{cat}/K_m of 2.0 × 10⁴ M^{-1} s^{-1} for BcsA-BcsB. For AcsA-AcsB, a k_{cat} of 67 s^{-1} and a k_{cat}/K_m of 5.0 × 10⁵ M^{-1} s^{-1} were determined (Table 1).

Termination: Strand Release. Strand release from the enzyme results in chain termination. The elution profiles, in addition to yielding information on steady-state kinetics (Figure 3, insets) and elongation (Figure 3) rates, also provide kinetic information on strand release. Each fraction eluting from the GPC column is not only characterized by its DOP as determined by elution time and MALLS but by its cellulose quantity, as determined by ¹⁴C scintillation spectrometry. Dividing the amount of glucose by the DOP yields the amount of reducing ends. Thus, reducing end content of each time

point can be quantified and thus the rate of strand release can be calculated. To assess the accuracy of this method, we also quantified reducing ends with bicinchoninic acid.[26] Figure 3C shows the time course of reducing ends released, as determined by both methods. Both methods yielded similar results. We then measured the rate of strand release as a function of varying UDP-Glc concentrations (Figure S2). The plot yields a V_{max} (k_{cat}) and the first-order rate constant of 1.2 × 10⁻³ s^{-1} for BcsA-BcsB and 3.1 × 10⁻⁴ s^{-1} for AcsA-AcsB.

Minimal Mechanism and Kinetic Simulation. A proposed mechanism for initiation, elongation, and termination is shown in Figure 5. The mechanism includes a fast elongation cycle and a slow initiation process. The right cycle depicts elongation, the processive addition of glucose. The left cycle involves termination (strand release) and initiation. Initiation involves UDP-Glc binding to E (k_1) followed by hydrolysis yielding glucose and UDP (k_2). This is followed by entry of the free glucose from the UDP-Glc binding site into the acceptor site located in the exit channel (k_4). The 4-hydroxyl of this new glucose is then poised to react with the next UDP-Glc, which binds at the UDP-Glc binding site (k_5). The new glycosidic bond is formed upon attack of the 4-hydroxyl of the "acceptor" glucose with the UDP-Glc (k_6). This rate constant includes the steps of both glycosidic bond formation as well as UDP release. For elongation to continue, the newly added glucose must translocate one glucose unit into the channel (k_4). Structural studies by Morgan et al.[14] indicate that translocation occurs concurrently with the movement of the finger helix motif, which contains the catalytic base. The authors contend that this shift may be facilitated either with the binding of UDP-Glc or spontaneously. Our mechanism supports the latter. Alter-
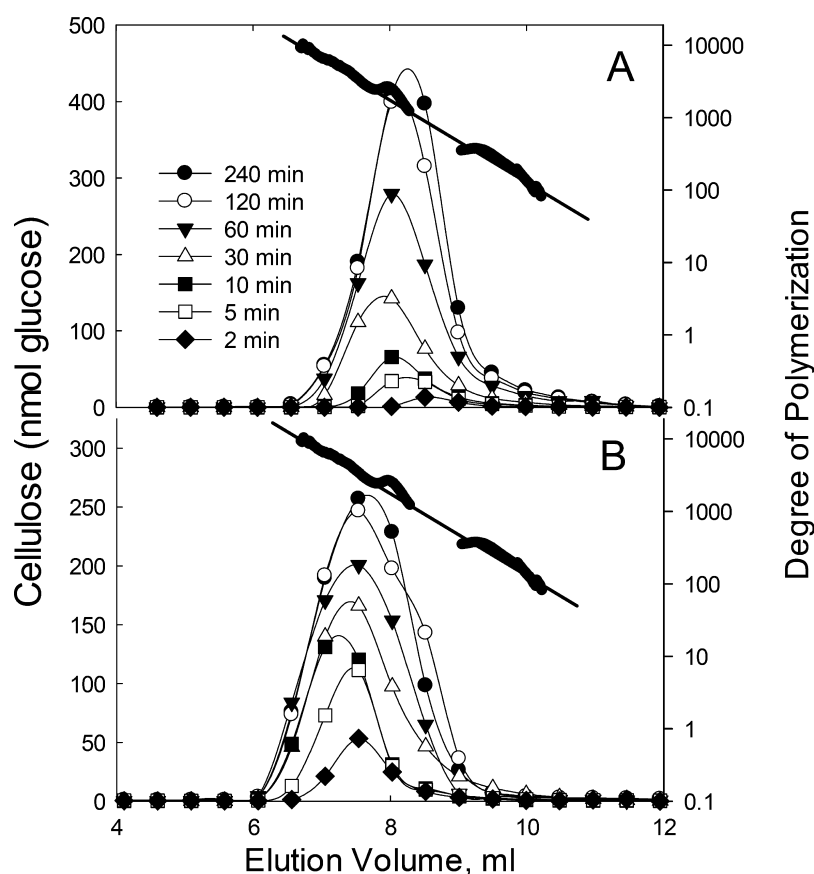
Figure 3. GPC elution profile of cellulose from BcsA-BcsB (A) and AcsA-AcsB (B). Aliquots were removed from enzymatic reaction mixtures at times as specified in the figures. Cellulose was synthesized from 0.5 nmol BcsA-BcsB or AcsA-AcsB with 5 mM UDP-^{14}C-Glc in a reaction volume of 1.0 mL, as described in Materials and Methods. The cellulose was dissolved in dimethylacetamide containing 8% LiCl (w/v), as described in Materials and Methods. Fractions (0.5 mL) were collected and quantified by scintillation spectroscopy. The column was calibrated by nonradioactive cellulose samples and their corresponding MALLS signals (shown as filled circles above elution profiles) with the DOP on the right axis. The inset in each graph plots the total cellulose from each sample vs time. (C) For reducing end quantification by bicinchoninic assay (●), cellulose was synthesized from 2 μM enzyme with 5 mM UDP-Glc in a reaction volume of 1.0 mL for the indicated time points. The cellulose was collected and the reducing ends were analyzed by bicinchoninic assay, as described in Materials and Methods. For reducing end quantification by GPC analysis (○), moles of glucose eluting from GPC were divided by the DOP (molecular weight) of the eluting cellulose in (A). Reducing ends are expressed as moles per mole of enzyme.

natively, translocation can proceed further than one glucose unit (k_3 and the left cycle shown in Figure 5A), forming free enzyme (E) thereby effectively terminating elongation and requiring reinitiation (Figures 5A and 4B).

With the mechanism shown in Figure 5 and measured rate constants (Table 1), kinetic simulations were performed. Tenua,[27] a modified version of Kinsim,[16] was used. Kinsim can only incorporate 10 steps, whereas Tenua has been modified to accommodate 100 steps. Even with this increase in steps, it cannot fully simulate elongation because it involves thousands of steps (see Figures S3 and S4 for the mechanistic details of such a simulation). For steady-state kinetics, velocity was measured (and simulated) as the rate of glucose incorporation in cellulose. We reasoned that the experimentally determined rate constants for strand release (k_3, Figure S2), the second-order rate constant between UDP-Glc and enzyme for elongation (k_5, Figure S1), and the rate of elongation (k_6, Figure S1), should be relatively accurate (Table 1). In contrast, measurements involving initiation (k_1 and k_2) would not be accurate. We reasoned that they would be lower estimates because it is not possible to measure the glucose incorporation rates from just initiation without the large amplification from elongation. Thus, the simulation would potentially provide

more accurate estimates of the rate constants. In addition, the rate of translocation (k_4) has been postulated to be not the rate-determining step on the basis of simulations by Knott et al.,[28] thus we have made this rate to be greater than k_6. Holding k_3, k_5, and k_6 to be equal to the measured rates, k_1 and k_2 were varied such that the steady-state rates were simulated. Figure 4 shows both actual rate data and the simulation using the values given in Table 1. In accord with the caveats mentioned above, the simulated rate constants for k_1 are much lower than the experimentally determined value.

Although steady-state kinetics was simulated, strand length or DOP could not be simulated due to the limitation of Tenua accommodating only 100 steps. We, thus, set up a mock simulation to determine whether the mechanism and rate constants can account for processivity. We increased rate constants (Table 1) such that Tenua would provide data on strand length. The simulation aimed at determining whether it was possible to simulate the size distribution of the cellulose (Figure 5C,D). The effect of increasing k_3 decreases the DOP (Figure 5C), whereas increasing k_4 increases the DOP (Figure 5D). Thus, the simulation shows that processivity of a cellulose synthase is directly influenced by the relative ratio of translocation by one glucose unit (k_4) (which results in
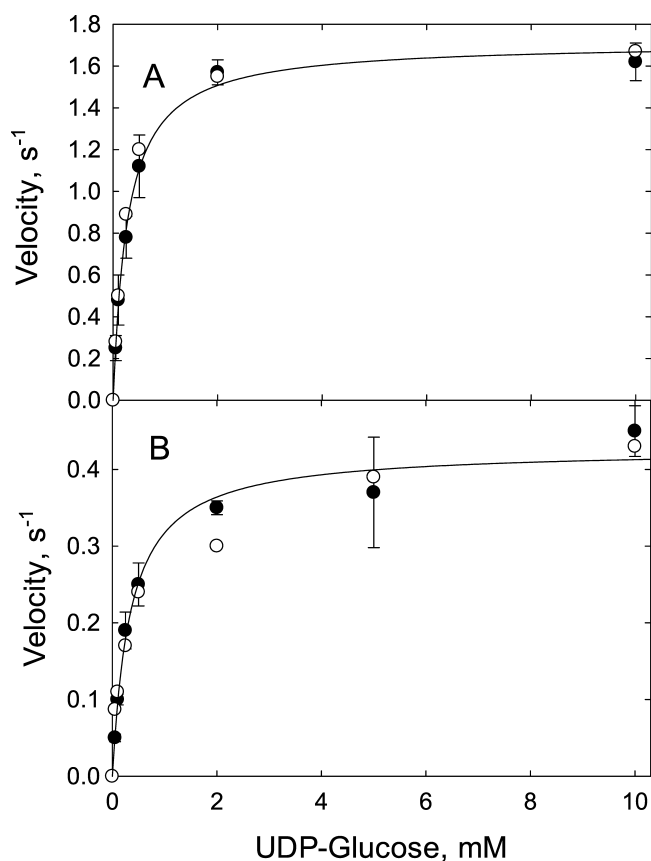
Figure 4. Steady-state kinetic analysis (●) and kinetic simulation (○) for AcsA-AcsB (A) and BcsA-BcsB (B). The rate of cellulose synthesis was measured in triplicate and shown with mean and standard deviation. Rates were measured by the enzyme-coupled assay as described in Materials and Methods and plotted as a function of UDP-Glc concentration. The measured rates are shown as filled circles. Using the experimentally determined kinetic constants given in Table 1, the steady-state rates were simulated by the Tenua software, as described in Materials and Methods and shown as open circles. The line shown in each plot is a curve fit to the Michaelis−Menten equation. The fit for AcsA-AcsB yields a k_{cat} of 1.7 ± 0.36 s^{-1} and a K_m of 0.27 ± 0.02 mM. For BcsA-BcsB, the fit yields a k_{cat} of 0.43 ± 0.17 s^{-1} and a K_m of 0.34 ± 0.07 mM.

elongation) or by translocation by greater than one glucose unit (k_3, strand release, termination).

■ DISCUSSION

Because of the insolubility of the product cellulose, kinetic characterization of cellulose synthases has been limited to steady-state kinetic studies where only the rate of product formation is measured.[12] No studies have probed the mechanism of initiation, elongation, or termination. The ability to solubilize the cellulose product by ionic liquids, resolve them by GPC, and analyze by MALLS, has allowed for the first time these parameters to be determined. This size distribution or length of each strand is most often expressed as DOP. DOP values are often determined from reducing end analysis[26] or by viscosity measurements.[5] Although GPC methods are available, which can provide such information,[4,29,30] to date, no studies have been performed on cellulose synthase, until now. Our study characterized all three phases of cellulose synthesis: initiation, elongation, and termination (strand release).

Table 1. Experimentally Determined Kinetic Values and Values Used in the Tenua Simulation

rate constant	AcsA-AcsB (measured)	AcsA-AcsB (steady-state simulation)	BcsA-BcsB (measured)	BcsA-BcsB (steady-state simulation)	BcsA-BcsB (processivity simulation)
k_1, M^{-1} s^{-1}	6100	200[b]	600	10[b]	3000
k_2, s^{-1}	nd[a]	0.035	nd	0.011	1.5
k_3, s^{-1}	2.1×10^{-4}	2.1×10^{-4}	1.2×10^{-3}	1.0×10^{-3}	0.4
k_4,[c] s^{-1}	nd	90	nd	16	5
k_5,[c] M^{-1} s^{-1}	5.0×10^5	5.0×10^5	2.0×10^4	2.0×10^4	1.4×10^6
k_6,[c] s^{-1}	67	70	12	12	100

[a]Not determined. [b]The experimental value is calculated from the slope of the Michaelis−Menten plot, as shown in Figure S1. The reaction of E in the unprimed form and in the primed form both contribute to this rate constant (k_{cat}/K_m) and thus is consistent with this value being higher than the simulated value. [c]The value for k_4 for translocation is modeled to be not the rate-limiting step (see Discussion) and thus is provided a higher estimated value.
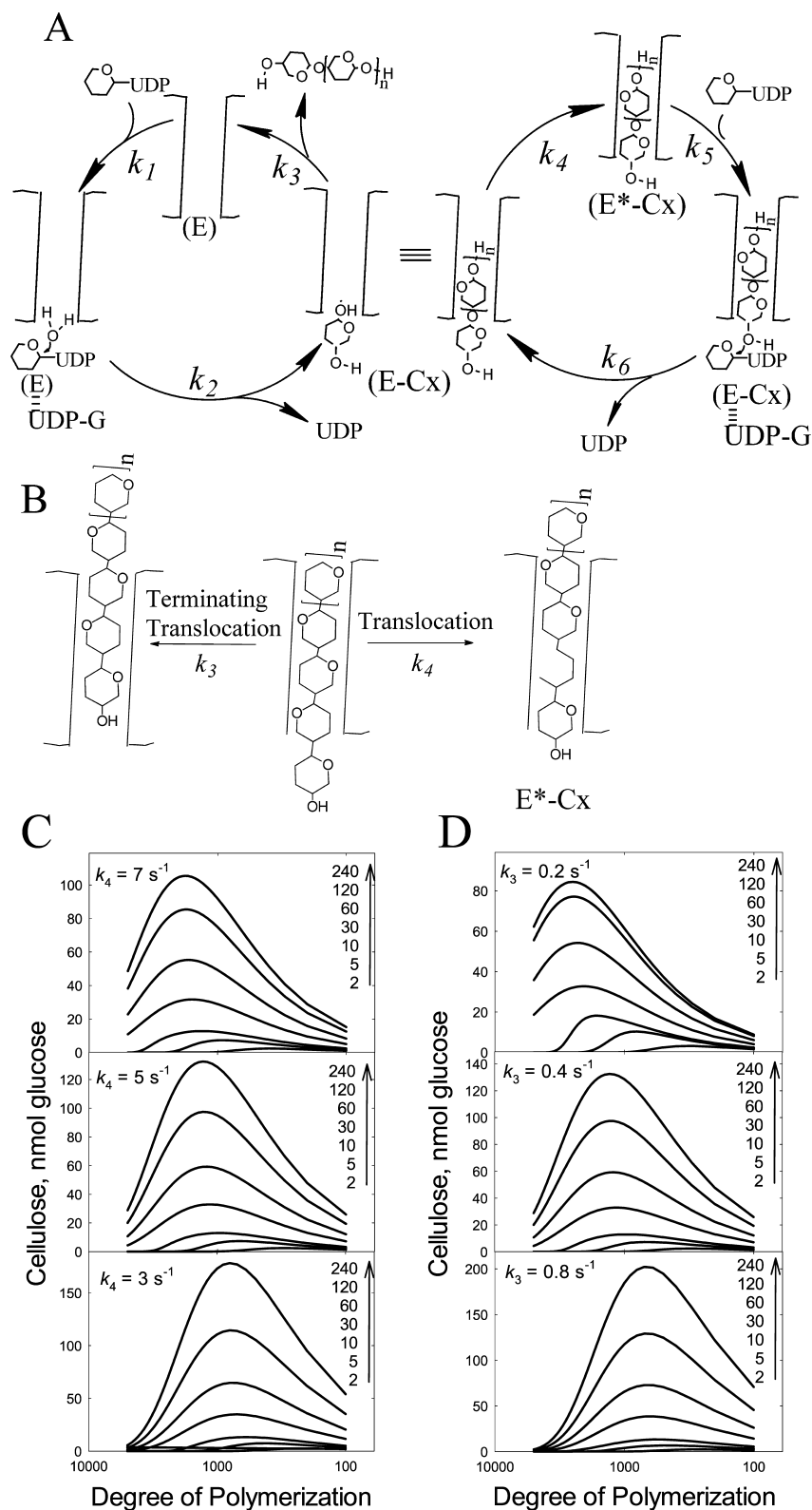
Figure 5. Proposed mechanism for cellulose synthase and simulation of DOP. (A) Elongation starts with the cellulose chain properly positioned in the channel (E*-Cx) for nucleophile attack of UDP-Glc by the nonreducing end. UDP-Glc binds to E*-Cx (k_5) to form the Michaelis complex. The attack of the 4-hydroxyl with the UDP-Glc forms the new glycosidic bond and E-Cx (k_6). The newly added glucose at the UDP-Glc binding site then must translocate into the channel by one glucose unit forming E*-Cx (k_4), which continues the cyclic process of elongation. Alternatively, translocation can proceed by more than one glucose unit resulting in strand release (k_3) or termination forming free enzyme (E). The free enzyme (E) can still have a cellulose chain attached; however, it is not within close proximity to react with the incoming UDP-Glc. Initiation involves binding of UDP-Glc to E (k_1). Hydrolysis of UDP-Glc yields glucose (k_2). This intermediate is similar to the intermediate formed during elongation where the newly added glucose must translocate from the UDP-Glc binding site into the channel (k_4). (B) A more detailed scheme. After addition of one glucose, the cellulose chain undergoes one translocation to form E*-Cx. Alternatively, the cellulose chain of E-Cx can undergo translocation greater

Figure 5. continued

than one glucose unit resulting in termination (k_3). (C, D) Simulated elution profiles based on the mechanism shown in (A) and (B). Because Tenua can only accommodate 100 steps, the rate constants were multiplied by 100 for the purpose of illustrating the importance of the k_4 to k_3 ratio in determining the processivity of the enzyme. (C) shows that increasing k_4 results in increased DOP. (D) shows that increasing k_3 results in decreased DOP. The Tenua input in regard to the mechanism and the rate constants used for the simulations are provided in Figures S4 and S5 and Table 1.

We found that for both bacterial cellulose synthases, primer-independent initiation occurred throughout the course of the reaction. Many glycosyl transferases operate by a primer-dependent mechanism for the initiation of polymer synthesis. The primer-dependent glycogen synthase requires a protein, glycogenin, for new strand synthesis.[31] For starch synthase, there are reports of primer-dependent and primer-independent mechanisms.[32−34] However, the apparent primer-independent enzymes may indeed be dependent upon endogenous primers that co-purified with the enzyme.[35] For plant cellulose synthase, Peng et al.,[36] working with crude membrane extracts, provided compelling evidence that sitosterol-β-glucoside acts as a primer. For bacterial cellulose synthase, the as-isolated enzyme already contains cellulose in the exit channel. Thus, it is similar to that of starch synthase on ambiguity of the involvement of primers. Using two different experimental approaches, our results show that both bacterial cellulose synthases have no requirement for a primer, which is in contrast to the plant system.[36] This was first demonstrated by our GPC analysis of the newly synthesized cellulose showing appearance of cellulose strands with low DOP throughout the time course of synthesis. We also showed that when UDP-^{14}C-Glc was used as the substrate, ^{14}C-Glc was detected at the reducing end of the cellulose strands. This can only occur by the utilization of UDP-Glc as the initiator of new strand synthesis. We also detected UDP-Glc hydrolase activity by the purified enzyme, which provides a mechanism for initiation. Nucleotide-sugar hydrolysis is a known activity of some glycosyl transferases.[22,23,37] However, incubations with ^{14}C-glucose and nonradioactive UDP-Glc did not result in ^{14}C-labeled reducing ends (not shown).

Once initiated, the enzyme enters the elongation phase that involves multiple cycles of glucose addition until the strand is released (termination). GPC analysis of the cellulose revealed not only a size maximum for each enzyme (∼23 000 for *G. xylinum* and ∼11 700 for *R. sphaeroides*), but analyzing the DOP as a function of time provided rates for elongation and for termination. Both of these rates were measured as a function of UDP-Glc concentration to obtain values of k_{cat}/K_m and k_{cat}. These values, in turn, were used to simulate both steady-state kinetics and also the processivity of the two bacterial enzymes. We were able to simulate steady-state kinetics and obtain estimated rate constants for rates that could not be measured for reactions involved in initiation. It is worth noting that the k_{cat} value we determined for BcsA-BcsB of 0.5 s^{-1} is much lower than that determined by Omadjela et al.[12] of approximately 90 s^{-1}. We have no apparent explanation for this discrepancy. However, we wish to point out that our value has been verified by three different assay methods: measuring the rate of UDP release through coupled enzyme assays, measuring the ^{14}C from insoluble cellulose formed, and also from data analysis from the GPC column. In addition, we measure the k_{cat} values for each new preparation of BcsA-BcsB and they are consistently within 20% of 0.5 s^{-1} (data not shown). Further supporting this k_{cat} value is that our value for AcsA-AcsB, a highly homologous enzyme, is close to 0.5 s^{-1} at a value of 1.7 s^{-1}. This value is very close to that obtained by Du et al.[38] of 2.9 s^{-1}.

In this work, we were also able to simulate the trends observed for processivity. Given the simulation software being limited to 100 steps (where the elongation cycle involved thousands of steps), we used parameters that would provide trends on DOP depending on the rate constants k_3 and k_4. The simulation clearly provided the relationship between trans-location by one glucose unit (k_4) versus strand release (k_3) and the impact on strand length. This is corroborated by the ratio of these two rates (k_4/k_3) for AcsA-AcsB (335 000) versus BcsA-BcsB (10 000). Indeed, the simulation shows that an increased ratio (translocation/strand release) increases the DOP and that is observed for these two enzymes.

In regard to the structural features that may account for difference in processivity, we reasoned that it would not be the active site. The UDP-Glc binding site or the active site in general for both bacterial enzymes is conserved. This is supported by the high homology in amino acid sequence. However, the cellulose strand for both enzymes processes through a well-defined channel.[12−15] Thus, interactions within this channel may impact both processivity and rate. Ongoing studies aim to determine structural determinants that impact processivity.

In summary, we have shown with purified enzymes that cellulose synthases have intrinsic processivities. Our results show that at least in vitro, initiation of synthesis is primer-independent. Initiation is most likely the rate-limiting step in catalysis. Finally, with the measured kinetic constants and our proposed mechanism, we have been able to simulate steady-state kinetics and even processivity. Ongoing studies aim at characterizing these parameters in plant cellulose synthases to understand structural factors that impact cellulose strand length.

◼ MATERIALS AND METHODS

Enzyme Expression and Purification. AcsA-AcsB was expressed homologously in *G. hansenii* and purified.[11] BcsA-BcsB was expressed heterologously in *Escherichia coli* and purified.[13] Protein concentration was determined by absorbance at 280 nm using molar extinction coefficients of 195 745 and 161 925 M^{-1} cm^{-1} for AcsA-AcsB and BcsA-BcsB, respectively.

Cellulose Synthesis and Characterization. Cellulose was prepared for GPC analysis by modification by phenyl isocyanate to form cellulose carbanilates.[39] A volume of 100 μL of phenyl isocyanate in 500 μL of pyridine was added to 1 mg of cellulose under a stream of dry argon gas. Samples were sealed in ampoules and rotated slowly at 70 °C for 48 h. Unreacted phenyl isocyanate was quenched with 1.2 mL of methanol. Samples were dried overnight at 40 °C under a stream of dry argon gas, dissolved in tetrahydrofuran, and filtered through 0.2 μm nylon filters (Millipore). GPC was performed with a KD-806M column (Shodex) using tetrahydrofuran. A specific refractive index (dn/dc) of 0.169 mL g^{-1}[14] was used for cellulose tricarbanilates in tetrahydrofuran. Enzymatic synthesis of cellulose from UDP-Glc was performed with UDP-[^{14}C]-Glc, as described by McManus et al.[11] All

reactions were performed at 30 °C or as specified in the figure legends. The synthesized cellulose was treated with 2% sodium dodecyl sulfate (SDS) and then solubilized with 8% LiCl (w/v) in dimethylacetamide for GPC analysis, as described previously.[25] Radioactivity was quantified by a Beckman Coulter LS6500 scintillation counter using ScintiVerse (Fisher Scientific) scintillation fluid.

KD-806M Column Calibration with Native Cellulose. Avicel (Sigma) and bacterial cellulose (*G. hansenii*) were dissolved in 8% LiCl (w/v) in dimethylacetamide. Injections of 100 μL of the solution were applied onto a KD-806M column (Shodex) and separated at a flow rate of 0.1 mL min^{-1}. Molecular weight determination was performed with a Dawn Helios II (Wyatt Technologies) MALLS detector coupled with a t-REx refractometer (Wyatt Technologies). A specific refractive index (dn/dc) of 0.0575 mL g^{-1} was used to calculate the molecular weight of cellulose in 8% LiCl in dimethylacetamide.[40]

Reducing End Analysis by 2-Aminobenzamide Labeling. Reducing end analysis was performed using 2-aminobenzamide (2AB) and fluorescent detection.[21] Cellulose was synthesized with either AcsA-AcsB or BcsA-BcsB using 1 mM UDP-[^{14}C]-Glc (2.63 mCi mmol^{-1}). Reactions were quenched by the addition of 2% SDS, and the cellulose was isolated by centrifugation and washed with water (2 × 1 mL) and then with dimethyl sulfoxide (DMSO) (2 × 1 mL). Cellulose was resuspended in 0.7 mL of DMSO and 0.3 mL of glacial acetic acid and modified, as described by Parekh et al.[21] The reaction mixture was tumbled gently at 60 °C for 12 h. The modified cellulose was isolated by centrifugation and washed with DMSO (2 × 1 mL), water (2 × 1 mL), ethanol (1 × 1 mL), and sterile water (1 × 1 mL). The cellulose was treated with 300 μL of 50 mM sodium acetate (pH 5.0) containing 200 U of cellulase (Worthington) and incubated at 37 °C for 24 h. Following digestion, the mixture was passed through a 3 kDa cut-off spin filter and the entire sample was injected onto a C$_{18}$ reversed-phase HPLC column (Supelco). The flow rate was 0.5 mL min^{-1} with 10 mM sodium acetate (pH 5.0) for 9 mL and then the solvent was changed to 10 mM sodium acetate, pH 5.0/acetonitrile (1/9) for 10 mL. Fractions of 0.5 mL were collected for scintillation counting.

Glucose Quantification. Glucose formation from the cellulose synthase reaction mixtures was measured using glucose oxidase and horseradish peroxidase, as per Tsuge et al.[41]

Reducing End Analysis by Bicinchoninic Acid. Cellulose was synthesized and reactions were quenched with 2% SDS, as described above. Solution A (0.512 M Na$_2$CO$_3$, 0.288 M NaHCO$_3$, and 5.0 mM bicinchoninic acid) and solution B (5.0 mM CuSO$_4$·5 H$_2$O and 12.0 mM L-serine) were mixed in a 1:1 ratio immediately prior to assaying to create a working solution. Volumes of 0.2 mL of working solution were added to 0.05 mL of water containing sample and vortexed. Samples were developed at 80 °C for 30 min and cooled in a water bath at 25 °C for 10 min. The samples were then centrifuged, and the absorbance of the supernatants was measured at 560 nm.[26] Glucose was used for the standard curve.

Tenua Simulations. Kinetic simulations were performed using Tenua,[16] a modified version of KINSIM.

■ ASSOCIATED CONTENT

ⓈSupporting Information

The Supporting Information is available free of charge on the ACS Publications website at DOI: 10.1021/acsomega.7b01808.

Double reciprocal plots (Figures S1 and S2) and schemes used for computer simulation of kinetics (Figures S3 and S4) (PDF)

■ AUTHOR INFORMATION

Corresponding Author

*E-mail: mxt3@psu.edu.

ORCID ⓘ

James D. Kubicki: 0000-0002-9277-9044

Ming Tien: 0000-0003-0257-2347

Notes

The authors declare no competing financial interest.

■ ACKNOWLEDGMENTS

■ REFERENCES

(1) Somerville, C. Cellulose synthesis in higher plants. *Annu. Rev. Cell Dev. Biol.* **2006**, *22*, 53–78.

(2) Youngs, H.; Somerville, C. Plant science. Best practices for biofuels. *Science* **2014**, *344*, 1095–1096.

(3) Youngs, H.; Somerville, C. Development of feedstocks for cellulosic biofuels. *F1000 Biol. Rep.* **2012**, *4*, 10.

(4) Dupont, A.-L.; Mortha, G. Comparative evaluation of size-exclusion chromatography and viscometry for the characterisation of cellulose. *J. Chromatogr. A* **2004**, *1026*, 129–141.

(5) Evans, R.; Wallis, A. F. A. Cellulose Molecular-Weights Determined by Viscometry. *J. Appl. Polym. Sci.* **1989**, *37*, 2331–2340.

(6) Hallac, B. B.; Ragauskas, A. J. Analyzing cellulose degree of polymerization and its relevancy to cellulosic ethanol. *Biofuels, Bioprod. Biorefin.* **2011**, *5*, 215–225.

(7) Hessler, L. E.; Merola, G. V.; Berkley, E. E. Degree of Polymerization of Cellulose in Cotton Fibers. *Text. Res. J.* **1948**, *18*, 628–634.

(8) Zhang, Y.-H. P.; Lynd, L. R. Determination of the number-average degree of polymerization of cellodextrins and cellulose with application to enzymatic hydrolysis. *Biomacromolecules* **2005**, *6*, 1510–1515.

(9) Schult, T.; Hjerde, T.; Optun, O. I.; Kleppe, P. J.; Moe, S. Characterization of cellulose by SEC-MALLS. *Cellulose* **2002**, *9*, 149–158.

(10) Lin, F. C.; Brown, R. M., Jr.; Drake, R. R., Jr.; Haley, B. E. Identification of the uridine 5′-diphosphoglucose (UDP-Glc) binding subunit of cellulose synthase in *Acetobacter xylinum* using the photoaffinity probe 5-azido-UDP-Glc. *J. Biol. Chem.* **1990**, *265*, 4782–4784.

(11) McManus, J. B.; Deng, Y.; Nagachar, N.; Kao, T.-h.; Tien, M. AcsA–AcsB: The core of the cellulose synthase complex from *Gluconacetobacter hansenii* ATCC23769. *Enzyme Microb. Technol.* **2016**, *82*, 58–65.

(12) Omadjela, O.; Narahari, A.; Strumillo, J.; Melida, H.; Mazur, O.; Bulone, V.; Zimmer, J. BcsA and BcsB form the catalytically active core of bacterial cellulose synthase sufficient for in vitro cellulose synthesis. *Proc. Natl. Acad. Sci. U.S.A.* **2013**, *110*, 17856–17861.

(13) Morgan, J. L. W.; Strumillo, J.; Zimmer, J. Crystallographic snapshot of cellulose synthesis and membrane translocation. *Nature* **2013**, *493*, 181−186.

(14) Morgan, J. L. W.; McNamara, J. T.; Fischer, M.; Rich, J.; Chen, H.-M.; Withers, S. G.; Zimmer, J. Observing cellulose biosynthesis and membrane translocation in crystallo. *Nature* **2016**, *531*, 329−334.

(15) Morgan, J. L. W.; McNamara, J. T.; Zimmer, J. Mechanism of activation of bacterial cellulose synthase by cyclic di-GMP. *Nat. Struct. Mol. Biol.* **2014**, *21*, 489−496.

(16) Barshop, B. A.; Wrenn, R. F.; Frieden, C. Analysis of Numerical-Methods for Computer-Simulation of Kinetic Processes: Development of KINSIM—a Flexible, Portable System. *Anal. Biochem.* **1983**, *130*, 134−145.

(17) Bae, S. O.; Shoda, M. Production of bacterial cellulose by *Acetobacter xylinum* BPR2001 using molasses medium in a jar fermentor. *Appl. Microbiol. Biotechnol.* **2005**, *67*, 45−51.

(18) Park, S.-M.; Yoon, S.-J.; Son, H.-J.; Lee, C.-Y.; Kim, H. S. Properties of Bacterial Cellulose Cultured in Different Carbon Sources. *Polymer* **2010**, *34*, 522−526.

(19) Harris, D.; DeBolt, S. Relative Crystallinity of Plant Biomass: Studies on Assembly, Adaptation and Acclimation. *PLoS One* **2008**, *3*, No. e2897.

(20) Tahara, N.; Tabuchi, M.; Watanabe, K.; Yano, H.; Morinaga, Y.; Yoshinaga, F. Degree of polymerization of cellulose from *Acetobacter xylinum* BPR2001 decreased by cellulase produced by the strain. *Biosci., Biotechnol., Biochem.* **1997**, *61*, 1862−1865.

(21) Parekh, R.; Ventom, A. Glycotechnology − an unambiguous technique for glycan analysis. *Am. Biotechnol. Lab.* **1995**, *13*, 9−10.

(22) Czabany, T.; Schmölzer, K.; Luley-Goedl, C.; Ribitsch, D.; Nidetzky, B. All-in-one assay for *β*-d-galactoside sialyltransferases: Quantification of productive turnover, error hydrolysis, and site selectivity. *Anal. Biochem.* **2015**, *483*, 47−53.

(23) Chavaroche, A. A. E.; van den Broek, L. A. M.; Springer, J.; Boeriu, C.; Eggink, G. Analysis of the polymerization initiation and activity of *Pasteurella multocida* heparosan synthase PmHS2, an enzyme with glycosyltransferase and UDP-sugar hydrolase activity. *J. Biol. Chem.* **2011**, *286*, 1777−1785.

(24) Dupont, A.-L. Cellulose in lithium chloride/N,N-dimethylace-tamide, optimisation of a dissolution method using paper substrates and stability of the solutions. *Polymer* **2003**, *44*, 4117−4126.

(25) McCormick, C. L.; Callais, P. A.; Hutchinson, B. H. Solution studies of cellulose in lithium-chloride and N,N-dimethylacetamide. *Macromolecules* **1985**, *18*, 2394−2401.

(26) Kongruang, S.; Han, M. J.; Breton, C. I. G.; Penner, M. H. Quantitative analysis of cellulose-reducing ends. *Appl. Biochem. Biotechnol.* **2004**, *113*, 213−232.

(27) Wachsstock, D. *Tenua*, 2017, http://bililite.com/tenua/.

(28) Knott, B. C.; Crowley, M. F.; Himmel, M. E.; Zimmer, J.; Beckham, G. T. Simulations of cellulose translocation in the bacterial cellulose synthase suggest a regulatory mechanism for the dimeric structure of cellulose. *Chem. Sci.* **2016**, *7*, 3108−3116.

(29) Yanagisawa, M.; Isogai, A. SEC−MALS−QELS study on the molecular conformation of cellulose in LiCl/amide solutions. *Biomacromolecules* **2005**, *6*, 1258−1265.

(30) Yanagisawa, M.; Shibata, I.; Isogai, A. SEC−MALLS analysis of cellulose using LiCl/1,3-dimethyl-2-imidazolidinone as an eluent. *Cellulose* **2004**, *11*, 169−176.

(31) Smythe, C.; Cohen, P. The discovery of glycogenin and the priming mechanism for glycogen biogenesis. *Eur. J. Biochem.* **1991**, *200*, 625−631.

(32) Boyer, C. D.; Preiss, J. Properties of citrate-stimulated starch synthesis catalyzed by starch synthase-I of developing maize kernels. *Plant Physiol.* **1979**, *64*, 1039−1042.

(33) Cao, H. P.; James, M. G.; Myers, A. M. Purification and characterization of soluble starch synthases from maize endosperm. *Arch. Biochem. Biophys.* **2000**, *373*, 135−146.

(34) Fujita, N.; Yoshida, M.; Asakura, N.; Ohdan, T.; Miyao, A.; Hirochika, H.; Nakamura, Y. Function and characterization of starch synthase I using mutants in rice. *Plant Physiol.* **2006**, *140*, 1070−1084.

(35) Schiefer, S.; Lee, E. Y. C.; Whelan, W. J. Requirement for a primer in in vitro synthesis of polysaccharide by sweet corn $(1 \rightarrow 4)$-*α*-D-glucan synthase. *Carbohyd. Res.* **1978**, *61*, 239−252.

(36) Peng, L.; Kawagoe, Y.; Hogan, P.; Delmer, D. Sitosterol-beta-glucoside as primer for cellulose synthesis in plants. *Science* **2002**, *295*, 147−150.

(37) Kelly, R. M.; Leemhuis, H.; Rozeboom, H. J.; van Oosterwijk, N.; Dijkstra, B. W.; Dijkhuizen, L. Elimination of competing hydrolysis and coupling side reactions of a cyclodextrin glucanotransferase by directed evolution. *Biochem. J.* **2008**, *413*, 517−525.

(38) Du, J.; Vepachedu, V.; Cho, S. H.; Kumar, M.; Nixon, B. T. Structure of the Cellulose Synthase Complex of *Gluconacetobacter hansenii* at 23.4 Å Resolution. *PLoS One* **2016**, *11*, No. e0155886.

(39) Henniges, U.; Kloser, E.; Patel, A.; Potthast, A.; Kosma, P.; Fischer, M.; Fischer, K.; Rosenau, T. Studies on DMSO-containing carbanilation mixtures: chemistry, oxidations and cellulose integrity. *Cellulose* **2007**, *14*, 497−511.

(40) Matsumoto, T.; Tatsumi, D.; Tamai, N.; Takaki, T. Solution properties of celluloses from different biological origins in LiCl center dot DMAc. *Cellulose* **2001**, *8*, 275−282.

(41) Tsuge, H.; Natsuaki, O.; Ohashi, K. Purification, properties, and molecular features of glucose oxidase from *Aspergillus niger. J. Biochem.* **1975**, *78*, 835−843.